HAL
archives-ouvertes.fr

Fire retardant benefits of combining aluminum hydroxide and silica in ethylene-vinyl acetate copolymer (EVA)

Rodolphe Sonnier, Amandine Viretto, Loic Dumazert, Marc Longerey, Sylvain Buonomo, Benjamin Gallard, Claire Longuet, Florian Cavodeau, Raphaël Lamy, Andrea Freitag

▶ **To cite this version:**

Rodolphe Sonnier, Amandine Viretto, Loic Dumazert, Marc Longerey, Sylvain Buonomo, et al.. Fire retardant benefits of combining aluminum hydroxide and silica in ethylene-vinyl acetate copolymer (EVA). Polymer Degradation and Stability, Elsevier, 2016, 128, pp.228-236. 10.1016/j.polymdegradstab.2016.03.030 . hal-02914565

HAL Id: hal-02914565
https://hal.mines-ales.fr/hal-02914565

Submitted on 25 May 2021

HAL is a multi-disciplinary open access archive for the deposit and dissemination of scientific research documents, whether they are published or not. The documents may come from teaching and research institutions in France or abroad, or from public or private research centers.

L'archive ouverte pluridisciplinaire **HAL**, est destinée au dépôt et à la diffusion de documents scientifiques de niveau recherche, publiés ou non, émanant des établissements d'enseignement et de recherche français ou étrangers, des laboratoires publics ou privés.

Fire retardant benefits of combining aluminum hydroxide and silica in ethylene-vinyl acetate copolymer (EVA)

Rodolphe Sonnier [a, *], Amandine Viretto [a], Loïc Dumazert [a], Marc Longerey [a], Sylvain Buonomo [a], Benjamin Gallard [a], Claire Longuet [a], Florian Cavodeau [a], Raphaël Lamy [b], Andrea Freitag [b]

[a] C2MA, Ecole des Mines d'Alès, 30100 Alès, France
[b] Elkem AS, Fiskaaveien 100, Kristiansand, Norway

A B S T R A C T

The flame retardancy of ethylene-vinyl acetate copolymer filled with metal hydroxides (aluminum hydroxide - ATH and magnesium hydroxide - MDH) and silica was investigated. Several composites containing only metal hydroxides or a combination of metal hydroxides and silica (ratio silica/hydrated filler = 0.18) were prepared and tested using pyrolysis-combustion flow calorimeter, thermogravimetric analysis and cone calorimeter at various heat fluxes. It was observed that silica provides benefits when the amount and other properties of the fillers allow the formation of an insulating mineral layer. In such cases, silica does not modify the first peak of heat release rate in cone calorimeter tests, but reduces or completely suppresses the breakdown of the insulating layer near the end of the combustion (assessed by the intensity of the second peak in the heat release rate as function of time). This effect is particularly obvious at lower heat flux, the insulating layer protects the underlying polymer, which is therefore not completely degraded.

Keywords:
Flame retardancy
Ethylene-vinyl acetate copolymer
Silica
Aluminum hydroxide

1. Introduction

Ethylene-vinyl acetate copolymer is one of the most studied polymers from the flammability point of view due to its huge use in the wire and cable industry. Most generally, EVA is flame retarded with high amount (up to 65 wt%) of hydrated mineral filler, especially aluminum hydroxide. Nevertheless, such high amounts negatively impact the mechanical properties. This is the main reason why much work has focused on the research of adjuvants able to improve the flame retardancy at lower filler loadings.

Another reason is that the protective layer formed by the accumulation of alumina on the upper surface of the material during burning breaks due to the pressure of pyrolytic gases, leading to an increase of heat release rate. This phenomenon can allow the flame to penetrate through the insulating layer of metal oxide to the underlying polymer. To maintain the integrity of the layer during the whole test, i.e. up to flame out, is a great challenge and combining ATH and other additives is considered as a potential solution.

Many compounds were used in combination with ATH or MDH to improve the flame retardancy of EVA: hydroxystannate [1], borate [2–5], expandable graphite [6], multiwalled carbon nanotubes [7,8], layered double hydroxide [9], crosslinked elastomeric particles [10–12], nitrogen-based additives (melamine) [13], organic or inorganic phosphorus-based additives [13–16], metallic oxides (including silica) [17–20] talc [21] and organomodified montmorillonite [7,22–29].

Several studies dealt with the effect of silica particles in EVA/ATH or EVA/MDH systems. Jiao and Chen [18] have replaced 2–10% of ATH by nanosilica in EVA containing 55 wt% of filler. The authors observed a decrease in Limiting Oxygen Index (LOI) but also a strong decrease in Peak of Heat Release Rate (pHRR) in cone calorimeter test (from 334 kW/m^2 for EVA/ATH 45/55 to 228 kW/m^2 for EVA/ATH/silica 45/53/2). A second peak of heat release rate occurring after 500 s is also reduced in presence of silica. In EVA filled with MDH, a small fraction of silica also allows decreasing the first peak of heat release rate (from 206 kW/m^2 with 60 wt% of MDH to 109 kW/m^2 with 52% of MDH and 8% of silica) [20]. The LOI increases (unlike in the previous study) and a V0 rating can be achieved in UL94 test. Nevertheless, an optimal content of silica

* Corresponding author.
E-mail address: rodolphe.sonnier@mines-ales.fr (R. Sonnier).

(8 wt%) is highlighted (at 12 wt%, the fire performances are strongly lowered). In both cases, the authors assumed that silica acts by reinforcing the residue.

Huang et al. have also incorporated 10 phr of silica into EVA/MDH (the filler loading was fixed at 55 wt%) [19]. The flame retardancy is not really improved (the LOI decreases, the pHRR in cone calorimeter decreases only slightly from 283 to 245 kW/m^2) but the authors observed an unexpected increase in Time-To-Ignition (TTI) from 126 to 298 s. Such an increase was not explained and was not observed by Jiao and Chen [18] or Fu and Qu [20].

Silica particles used in this study, called SIDISTAR, have already been investigated as adjuvant to improve the flame retardancy of various polymers, as polyamides or styrene-butadiene rubber (SBR) filled with ATH [30–33]. Schmaucks and Friede have shown that the effect of SIDISTAR on the flame retardancy of polyamides depends on the polyamide types [30]. Gallo et al. have studied SBR filled with high amount of different ATH and SIDISTAR [31]. They showed that SIDISTAR improves the flame retardancy according to different criteria (as limiting oxygen index and time-to-ignition) but the extent of the improvement depends on the ATH type. While the same ATH as in our study was used, the results of this work will be extensively discussed in the following. The authors have proved that SIDISTAR hinders the release of pyrolytic gases using gravimetric gas sorption measurements. Then the thermal stability of the material is enhanced and the ignition is delayed. Moreover, the authors observed that SIDISTAR improves the residual protective layer formed during cone calorimeter tests and the second pHRR (generally assigned to the mineral layer breakdown) is strongly reduced.

In many studies, the improvement of performances due to the combination of ATH and other mineral fillers is only observed but not really explained. Moreover, the conditions for which this improvement is observed are not always studied. For example, the cone calorimeter tests are often carried out at only one external heat flux.

In this study, we show that silica provides a new property (i.e. a more cohesive residue) at low loading in EVA filled with high contents of hydrated mineral fillers. This conclusion is close to that of Gallo et al. [31] but based on additional characterization tests.

2. Materials and methods

Ethylene-vinyl acetate copolymer (Alcudia PA-440 supplied by Repsol) contains 28 wt% of vinyl acetate. ATH and MDH are respectively Martinal LEO 104 and Magnifin H10 (provided by Martinswerk Gmbh). The particles mean size is 1.7–2.1 μm for ATH and 0.8–1.1 μm for MDH (data from manufacturer).

Silica particles, called SIDISTAR T120, were kindly provided by Elkem AS (Norway). SIDISTAR® T120 consists of spherically shaped particles with median diameter of 180 nm and a specific surface area of 25 m^2/g. SiO_2 content is 97%.

Formulations were extruded using a co-rotating twin-screw extruder (Clextral BC21, length 900 mm, speed 200 rpm, screw diameter 25 mm, temperature 60–165 °C). The obtained pellets were injection molded (Krauss Maffei 180-CX 50 t, T = 140–160 °C, mold temperature = 30 °C) to obtain square specimens (100 × 100 × 4 mm^3). True filler content was calculated from the experimental residue measured using thermogravimetric analysis assuming that EVA is fully degraded, ATH and MDH release 35 and 31 wt% of water respectively and silica is inert. For formulations containing hydrated fillers and silica the weight ratio silica/ATH (or MDH) was fixed at 0.18. MDH51 S9 exhibits a slightly lower filler content than its counterpart MDH60 (55 versus 60 wt%). Therefore the comparison between both formulations is only approximate.

All compositions are listed in Table 1.

Thermogravimetric analyses (TGA) was performed using a Setsys Evolution apparatus (Setaram). 10 (±2) mg-samples were heated under nitrogen flow (100 mL/min) at a heating rate equal to 1 °C/s from ambient to 900 °C after a first isotherm at 30 °C lasting 30 min.

Fuel production was investigated using a pyrolysis combustion flow calorimeter (PCFC from Fire Testing Technology, UK) which was developed by Lyon and Walters [34]. The sample (3 ± 0.5 mg) was heated from 80 to 750 °C at 1 °C/s in a pyrolyzer under nitrogen flow and the degradation products were sent to a combustor where they are mixed with oxygen in excess at 900 °C. In such conditions, these products were fully oxidized. Heat Release Rate (HRR) was then calculated by oxygen depletion according to Huggett's relation (1 kg of consumed oxygen corresponds to 13.1 MJ of released energy) [35]. Very small samples (several milligrams) could be analysed using PCFC.

In such an apparatus, some fire retardant effects (such as the barrier effect of gas phase flame inhibition) cannot be effectively observed [36]. Therefore fire behavior was also studied using a cone calorimeter (Fire Testing Technology). A horizontal sample sheet of 100 × 100 × 4 mm^3 was placed at 25 mm below a conical heater and insulated by rock wool. The samples were exposed to various heat fluxes (25, 35, 50 and 75 kW/m^2) in well-ventilated conditions (air rate 24 L/s) in the presence of a spark igniter to force the ignition. HRR was determined according to oxygen depletion (Huggett's relation) as in PCFC. This test was performed according to the ISO 5660 standard. Each flame retarded blend was tested at 35 kW/m^2. ATH60 and ATH51 S9 blends were also tested at other heat flux (25, 50 and 75 kW/m^2). For these formulations, the temperature of the upper surface was measured during cone calorimeter test using an infrared camera (Optris). The distance between the specimen and the cone was increased to 60 mm to allow a correct measurement, but the heat flux was kept equal to 35 kW/m^2.

ATH60 and ATH51 S9 blends were also characterized by "epiradiator test" instrumented with an infrared pyrometer (Optris). 70 × 70 × 4 mm^3 specimens were continuously exposed to a 500 W radiator (diameter 10 cm, made of opaque quartz). The heat flux on the upper surface of the specimen was measured equal to 37 kW/m^2. Specimens were embedded in aluminum foil and placed on a grid located 34 mm under the bottom of the epiradiator. The grid was perforated in its center. The infrared pyrometer was placed perpendicularly to the surface below the specimen in order to measure the temperature of the aluminum foil through the grid hole. The aluminum foil was thin and covered by a thin graphite layer (emissivity close to 1). Therefore the measured temperature with the pyrometer can be considered as the true temperature of the lower surface of the specimen. After burning, the epiradiator was removed and the residue was allowed to cool down to room temperature. Then the epiradiator was repositioned above the residue and the temperature was recorded again. Such a procedure allows assessing the insulating properties of the residue without destroying it.

Viscosity measurements were carried out in dynamic mode at 150 °C using 1% strain and a frequency ranging from 10^{-1}–10^2 rad s^{-1} (ARES, Rheometric Scientific). All samples were characterized in triplicate and mean values are shown.

Oedometric compression test on some residues collected from cone calorimeter test was carried out according to the procedure developed and proposed by Cavodeau et al. [37]. In this work, oedometric compression tests were carried out on residues from EVA filled with ATH and other mineral fillers after cone calorimeter test. The slope of compression was found to be correlated to the appearance of the second peak of heat release rate. This second

Table 1
Composition of the studied formulations.

Formulations	EVA content (wt%)	ATH content (wt%)	MDH content (wt%)	Silica content (wt%)	True filler content[a] (wt%)
ATH20	80	20	0	0	20.9
ATH17 S3	80	17	0	3	20.4
ATH40	60	40	0	0	39.7
ATH34 S6	60	34	0	6	38.6
ATH60	40	60	0	0	59.8
ATH51 S9	40	51	0	9	59.4
MDH60	40	0	60	0	60.1
MDH51 S9	40	0	51	9	55.0

[a] Calculated from residue measured using thermogravimetric analysis.

pHRR is believed to be due to the breakdown of the insulating mineral layer: when this layer is broken, the barrier effect is vanished and the degradation rate increases. Briefly a mass of 10 g of product was introduced in the non-deformable cell for each test. The force was applied using a piston. The compression was carried out using a Z010 Material Testing Equipment (Zwick) with a 10 kN sensor, at a speed of 10 mm/min 3 tests were carried out for each tested formulation. The reproducibility was very good (the standard deviation on the slope of compression curve was less than 2 daN). More details can be found elsewhere [37].

3. Results

3.1. Thermal degradation at small scale

Fig. 1 shows the mass loss and the heat release rate versus the temperature measured using TGA and PCFC, respectively, for all studied formulations. Table 2 summarizes the main data. The degradation occurs in two main steps. The first one corresponds to the water release from ATH or MDH and to the first degradation step of EVA (release of acetic acid). Both phenomena overlap in the same range of temperature (300–450 °C – it must be noticed that the water release from ATH occurs at higher temperature than in most studies due to the high heating rate – 1 K/s). The second degradation step occurs between 450 and 550 °C and corresponds to the complete degradation of EVA. The residue allows calculating the true filler content (see Table 1) in good agreement with expected content (except for MDH51 S9 – the true filler content is slightly lower than the expected one (55 versus 60 wt%).

Heat release rate curves show two pHRR corresponding respectively to the first and the second steps of EVA degradation. The main peak and the Total Heat Release (THR) are proportional to the EVA content. The Effective Heat of Combustion (EHC) is calculated using residue content measured in TGA and total heat release measured in PCFC. It decreases due to the dilution of fuels by non-combustible gas (i.e. water from hydrated fillers). A slightly higher value is observed for MDH51 S9 due to filler content lower than expected as already noted in Materials section. The temperature of the main pHRR (TpHRR) is constant (around 485 °C). There is no significant difference when a fraction of hydrated fillers is replaced by silica.

All these results show that silica does not modify the degradation pathway of EVA or the water release kinetics from hydrated fillers. This result is not in agreement with those reported by Gallo et al. [31]. These authors observed a slight increase (+15 °C) of thermal stability for SBR filled with 120 phr of ATH and 20 phr of SIDISTAR.

3.2. Cone calorimeter test: influence of composition

Table 3 summarizes the main data measured using cone calorimeter at 35 kW/m^2. Fig. 2 shows the heat release rate curves for all formulations. As observed, the incorporation of fillers allows increasing time-to-ignition due to the release of water through endothermic decomposition, which cools the surrounding polymer and dilutes the fuel in gas phase. Nevertheless, at low filler loading, the TTI decreases (in comparison to pure EVA). This result may be related to higher heat absorption at the surface [38] or to an increase of viscosity preventing the heat transfer from the surface to the bulk. It can be also noted that MDH is more effective than ATH at increasing TTI (please compare TTI of ATH60 and MDH60). This may be a result of the range of water release temperatures. ATH releases water at relatively low temperature when pyrolysis has not started yet. In contrast, MDH releases water during the first decomposition step of EVA. Therefore, water not only cools the condensed phase, but also dilutes fuel in the gas phase, keeping the fuel below the lower flammability limit. Finally, the replacement of hydrated filler by silica decreases TTI, particularly at high filler

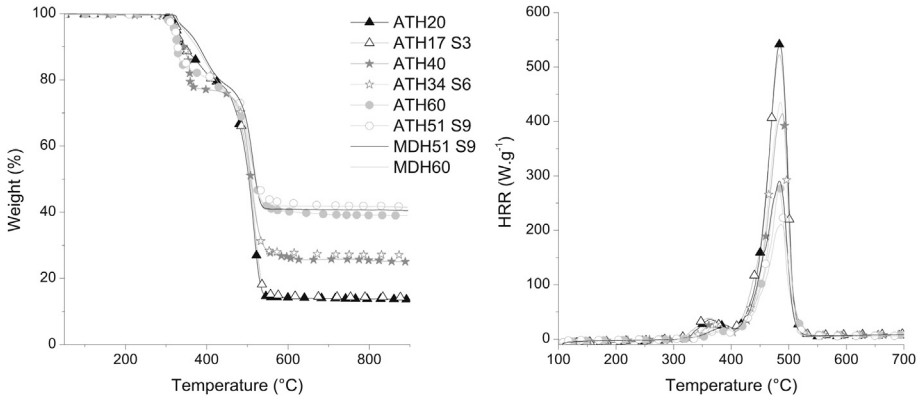

Fig. 1. Mass loss (left) and heat release rate (right) curves for the studied formulations.

Table 2
Main results from PCFC and TG analyses for the studied formulations.

Formulations	pHRR (W/g)	TpHRR (°C)	THR (kJ/g)	Residue content (%)	EHC (kJ/g)
EVA	756	487	36.0	0	36.0
ATH20	540	484	27.5	13.6	31.8
ATH17 S3	519	484	27.7	14.3	32.3
ATH40	411	489	21.5	25.8	29.0
ATH34 S6	432	485	21.1	27.1	28.9
ATH60	273	485	13.9	38.9	22.7
ATH51 S9	272	481	13.7	41.7	23.5
MDH60	231	483	13.0	41.5	22.1
MDH51 S9	293	484	15.7	40.5	26.4

Table 3
Main results from cone calorimeter tests at 35 kW/m^2 for the studied formulations.

Formulations	TTI (s)	pHRR (kW/m^2)	EHC (kJ/g)	Residue (wt%)	THR (kJ/g)
EVA	59	765	35.1	0	35.1
ATH20	52	600	33.4	14.9	28.1
ATH17 S3	47	568	32.9	15.8	27.8
ATH40	64	394	28.8	30.2	20.0
ATH34 S6	65	370	29.0	28.7	20.5
ATH60	89	212	22.9	41.3	13.2
ATH51 S9	76	187	24.9	47.2	12.9
MDH60	137	238	24.6	45.0	13.0
MDH51 S9	120	252	26.8	41.6	15.2

of SIDISTAR does not modify greatly the first pHRR of SBR filled with ATH (348 kW/m^2 versus 361 kW/m^2 for SBR/ATH without SIDISTAR) [31]. In the case of MDH-based formulations, as already mentioned, the filler content is slightly lower for MDH51 S9. Therefore, the comparison between MDH60 and MDH51 S9 must be considered with caution. Nevertheless, even if there is no modification of pHRR, HRR curves change in presence of silica. In particular, silica leads to a complete disappearance of the second peak of heat release rate in the case of EVA filled with high amount of ATH (please compare ATH60 and ATH51 S9). These formulations are the only ones exhibiting a curve typical of the so-called barrier

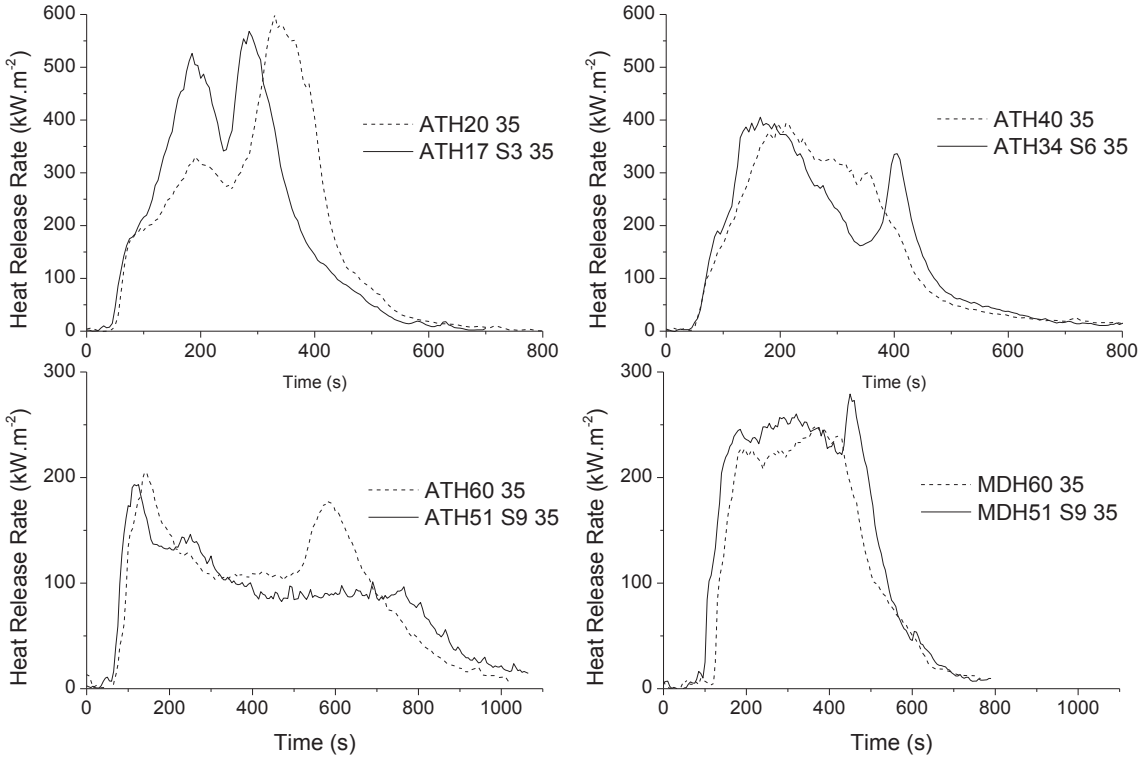

Fig. 2. Heat release rate curves for the studied formulations at 35 kW/m^2

loading. In their article, Gallo et al. have observed that SIDISTAR increases time-to-ignition in cone calorimeter test for SBR filled with ATH [31]. This increase was explained by the slowdown of pyrolytic gases diffusion into the material.

The peak of heat release rate is also reduced in presence of fillers, but the replacement of ATH by silica does not lead to further improvement. Gallo et al. have also observed that the incorporation effect [39] (i.e. the formation of a protective layer insulating the underlying polymer from the flame). This point will be discussed later. It must be noted that the second peak of heat release rate is generally assigned to the breakdown of the barrier layer in formulations exhibiting such a typical curve.

The effective heat of combustion decreases in presence of hydrated fillers due to the release of water, which dilutes the fuel. The

values are close to those obtained using PCFC and TGA (see Table 2). According to the uncertainties on these data (±2 kJ/g), the combustion efficiency can be considered close to 1 for all formulations.

The residue content increases when incorporating fillers. It is generally close to the values measured by TGA, i.e. to the mineral residue without any significant charring. Only the experimental residue of ATH51 S9 is significantly higher than the expected one (47.2 versus 41.5 wt%, i.e. a gain of 5.5 wt%). Such a discrepancy can be assigned to charring or to an incomplete degradation of the material. While no charring is observed (the surface is white or grey, but not black), this result evidences that the barrier layer formed during the burning protects the underlying polymer (incomplete degradation). It is worth mentioning that silica also influences the heat release rate curve of this formulation by suppressing the second peak of heat release rate (i.e. the breakdown of the barrier layer).

Total heat release depends on effective heat combustion and residue content. While fillers allow decreasing the former and increasing the latter, total heat released is significantly reduced when incorporating filler. Silica modifies neither EHC nor residue content, and the THR remains constant when ATH or MDH are replaced by silica. The increase in residue content in the case of ATH51 S9 is not high enough to significantly impact the THR value (taking into account the uncertainties, ± 2 kJ/g).

The main effect of silica particles (i.e. the decrease in the second peak of heat release rate for EVA filled with high amount of ATH) is in good agreement with Jiao and Chen's study [18]. Gallo et al. [31] have also noted a decrease of the second peak of heat release rate (from 502 to 327 kW/m^2) for SBR filled with the same ATH and SIDISTAR. In the study of Fu and Qu concerning EVA/MDH [20], most of formulations did not exhibit a HRR profile typical of a barrier effect from the mineral layer, as in our study. Only some formulations with a sufficient fraction of silica showed such a profile (tested at 35 kW/m^2). The second peak of heat release rate is small at an optimal range of silica (5–8 wt%) but strongly increases at higher content (12 wt%). The reason why we do not observe the same profile is unclear. This difference may depend on the grade of mineral particles used.

3.3. Cone calorimeter test: influence of heat flux

EVA copolymers filled with 60 wt% of ATH or 51 wt% of ATH and 9 wt% of silica (called ATH60 and ATH51 S9) were tested using different heat flux (25, 35, 50 and 75 Kw/m^2). Table 4 summarizes the main results. Fig. 3 shows the heat release rate curves. High heat flux obviously leads to an earlier ignition and a higher first peak of heat release rate. EVA filled only with ATH exhibits a slightly higher TTI. There is no significant and systematic difference in the first pHRR between both formulations.

However a great difference is observed concerning the second peak of heat release rate, related to the breakdown of the insulating mineral layer. In the case of ATH60, this peak is always observed, whatever the heat flux. This second peak is almost as high as the first one (and even higher, at 25 kW/m^2). On the contrary, in the presence of silica (ATH51 S9), this second peak is only observed at 75 kW/m^2, but totally disappears at lower heat flux.

Fig. 4 shows the difference between the expected residue content in thermogravimetric analysis and the measured one for different heat flux and both formulations. At high heat flux (75 kW/m^2), the measured residues are similar to the expected ones, evidencing that the breakdown of the layer allowed the full decomposition of the polymer. At lower heat flux, the measured residues are higher than the expected ones, particularly for ATH51 S9. At 25 kW/m^2, the measured residue is around 10 wt% higher than expected. Considering that the fraction of EVA is 40 wt%, it means that almost 25 wt% of EVA is not volatilized. While EVA is decomposed at a temperature much higher than ATH, it is reasonable to consider that EVA rather than ATH is not fully degraded. This result is in good agreement with the strong decrease in EHC and THR observed for this formulation (respectively, 18.7 and 8.5 kJ/g versus 24.5 and 14 kJ/g at the highest heat flux). In all other cases, the fraction of non-degraded EVA remains too small to impact significantly EHC and THR (taking into account the uncertainties on these values, i.e. ± 2 kJ/g). Fu and Qu [20] have also observed a slight decrease in EHC when incorporating silica into EVA flame retarded with hydrated fillers (MDH). Nevertheless, they did not indicate the residue content, and they did not assign the decrease of EHC to an incomplete degradation of EVA.

It must also be noted that the measured residues of ATH60 is higher than the expected ones at 25 and 35 kW/m^2 despite the occurrence of the second pHRR (related to the layer breakdown). But the fraction of EVA, which is not fully degraded, is significantly lower.

To prove that the second peak of heat release rate is due to the breakdown of the mineral layer, additional experiment was carried out with instrumented epiradiator. Fig. 5 shows the temperature of the lower surface of ATH60 and ATH51 S9 and their residues. The heating of the lower surface for both formulations is similar during the first part of the test (up to 500 s). Above 500 s, the temperature increases faster and reaches a higher value for ATH60 in good agreement with cone calorimeter tests (360 versus 300 °C for ATH51 S9). Indeed, a higher heat release rate at the end of the test and the breakdown of the layer (as observed in cone calorimeter tests) may explain that the lower surface reaches a higher temperature.

The same test on the residue confirms that the mineral layer was damaged during the burning of ATH60. Indeed, the temperature of the lower surface of the residue increases instantly while for the ATH51 S9 the temperature of the residue increases only after 40–50 s. This could mean that in the former case, the heating front reaches the lower surface very quickly, probably because of some cracks. Moreover, the heating rate is much lower for ATH51 S9.

Table 4
Main results from cone calorimeter tests for ATH60 and ATH51 S9.

Heat flux (kW/m^2)	TTI (s)	pHRR 1 (kW/m^2)	pHRR 2 (kW/m^2)	EHC (kJ/g)	Residue (%)	THR (kJ/g)
ATH60						
75	27	301	227	23.4	38.8	14.1
50	49	243	159	23.6	41	13.7
35	89	212	181	22.9	41.3	13.1
25	133	144	135	24.8	45.5	12.9
ATH51 S9						
75	25	322	202	24.5	41.9	14
50	51	253	/	25	45.7	13.4
35	76	187	/	24.9	47.2	12.9
25	123	111	/	18.7	51.5	8.5

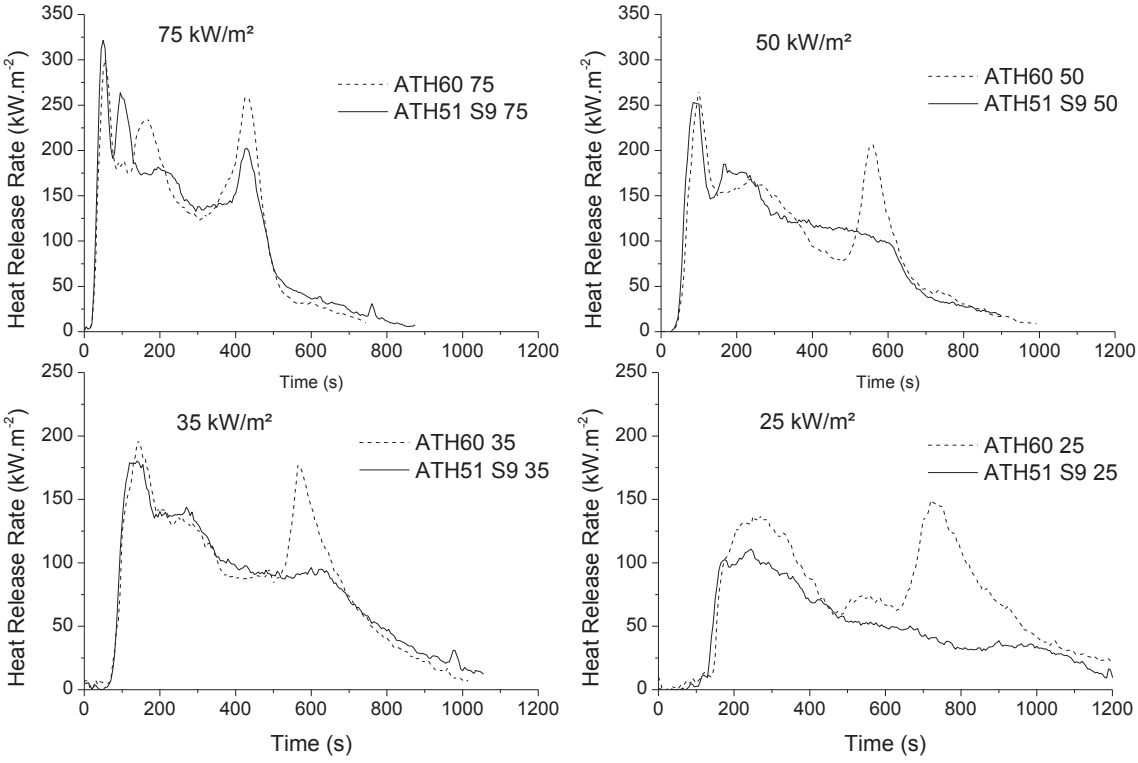

Fig. 3. Heat release rate curves for ATH60 and ATH51 S9 at various heat fluxes.

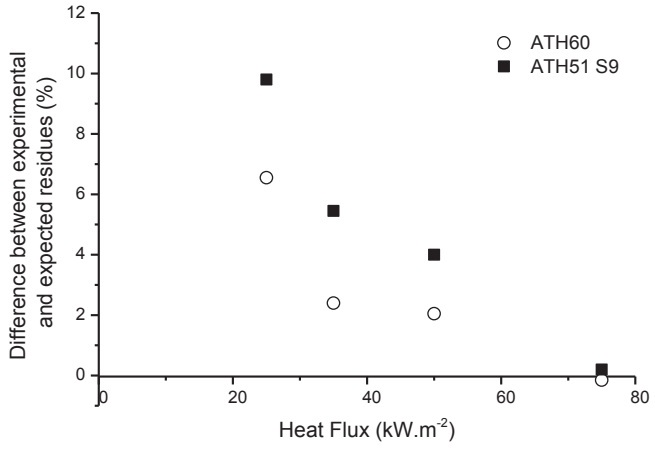

Fig. 4. Difference between measured and calculated residues for ATH60 and ATH51 S9 for various heat fluxes.

Therefore, even if the same temperature (around 300 °C) is reached for both residues, the peak value is reached after only 200 s for the residue from ATH60 versus around 700 s for the residue from ATH51 S9. All these results confirm that silica particles reinforce the residue and limit its damage, maintaining its insulating properties.

Upper surface temperature during cone calorimeter test was also recorded using an infrared camera for ATH60 and ATH51 S9. For this test, the heat flux was fixed at 35 kW/m^2 and the distance between the cone and the sample was increased to 60 mm. The distance between the sample and the spark igniter was also increased, and this may be the reason, why the TTI are not exactly the same as those obtained previously. As shown in Fig. 6, several changes in heating rate can be noticed for both composites. Just after 200 °C, the heating rate increases. This is quite surprising because ATH release water from 200 °C. Nevertheless, some works have already observed that water release can lead to bubbling and to an increase in heating rate (due to a change of surface optical properties) [40,41]. The temperature reaches a quasi-plateau around 350 °C. This plateau can be related to the first step of EVA degradation (release of acetic acid). Finally, ignition occurs at 500 °C, which is the temperature of the second peak of degradation (as measured in PCFC).

There is no difference between both composites except the TTI which is slightly delayed for ATH60, as already noticed. This is due to a slightly longer plateau at 350 °C, probably because the cooling of the material through the endothermic decomposition of ATH is slightly more important for this formulation. After ignition, the temperature becomes stable close to 700 °C, i.e. a much higher temperature compared to that of EVA pyrolysis, because the mineral layer (alumina and silica) can be heated without degradation. This temperature is stable up to the decrease of the flame (see Fig. 6). During the period 500–700 s corresponding to the breakdown of protective layer, no further difference is noted. Therefore such a breakdown has no effect on the surface temperature.

4. Discussion

According to the results presented above, silica can be considered as an additive improving the flame retardancy of EVA filled with high content of ATH. More precisely, silica does not modify significantly the first peak of heat release rate but leads to a strong decrease (and even disappearance) of the second peak corresponding to the breakdown of the barrier layer. In the following we attempt to discuss only these two phenomena. Heat release rate curves are complex (with several other small peaks) and further work is needed to explain in detail their full profiles.

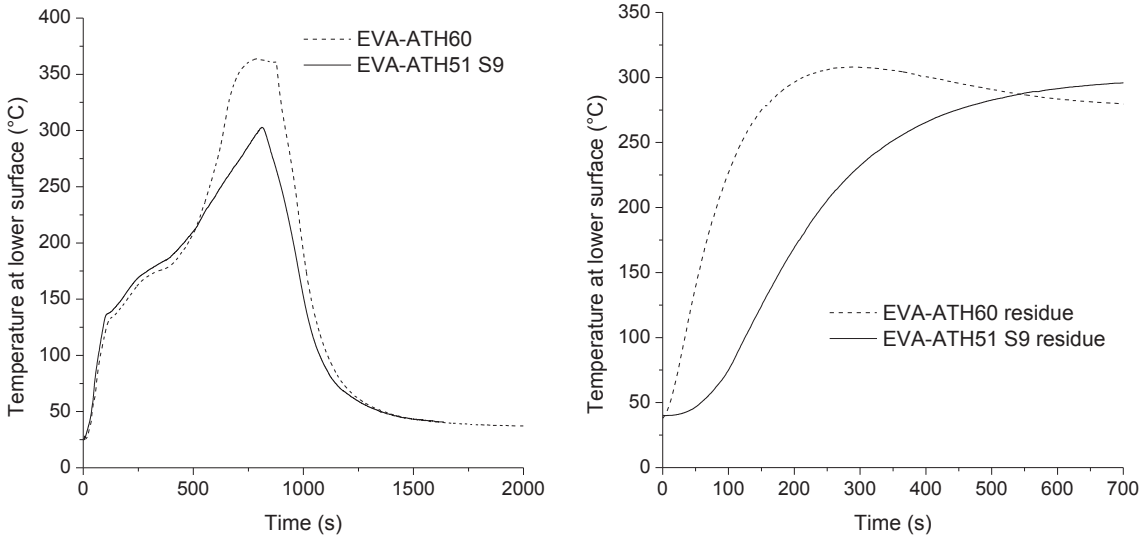

Fig. 5. Temperature of the lower surface during instrumented epiradiator test – Left, for ATH60 and ATH51 S9 formulations; right, for corresponding residues.

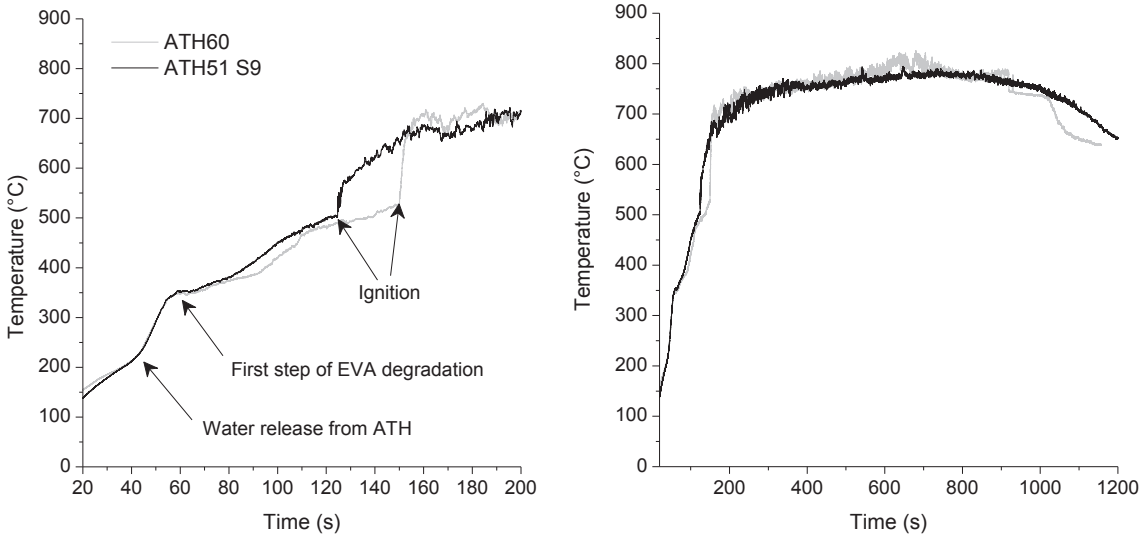

Fig. 6. Temperature of the upper surface during cone calorimeter test at 35 kW/m^2 for ATH60 and ATH51 S9; left: details during the first 180 s, right: the whole curves.

4.1. Influence of rheological properties

Some authors have shown that viscoelastic properties play an important role in the heat release rate measured using a cone calorimeter test. Kashiwagi et al. have highlighted the influence of matrix viscosity on the accumulation of silica on the top surface of PP/silica [42,43]. In another study, they showed that the formation of a protective network in PS filled with clays or multiwalled carbon nanotubes (MWCNT) was strongly dependent on the viscosity [44]. More recently, Batistella et al. have evidenced that peak of heat release rate was correlated to the elastic modulus G′ in EVA filled with various hydrated minerals (ATH, MDH, boehmite, alumina, kaolinite) [45]. Courtat et al. have observed the same relation between viscoelastic properties and pHRR in PP filled with medium content (5–20 wt%) of various silicas [41]. More precisely, these two last studies showed that pHRR decreases faster when G′ increases (regime I) up to a threshold (reached when $G'_{composite}$ is around five times G'_{EVA}). Above this threshold, pHRR remains constant even if G′ increases (regime II). Of course, all these studies are based on the measurement of rheological properties at processing temperature while the temperature of the condensed phase in cone calorimeter is changing, heterogeneous and reaches higher values (up to pyrolysis temperature).

Fig. 7 plots the change in pHRR with G′ for our composites and those studied by Batistella et al. [45]. It must be noted that the cone calorimeter tests were not carried out at the same heat flux in both studies. Nevertheless, our composites exhibit the same tendency as those studied by Batistella et al. a fast decrease in pHRR when G′ increases followed by a plateau for which pHRR is constant whichever G′ value.

This result confirms that the first pHRR is controlled by the viscoelastic properties. While silica does not lead to a strong increase in G′ value, the pHRR of EVA filled with ATH is not significantly modified, even if these composites are plotted in regime I in Fig. 7.

Interestingly, EVA filled with MDH and silica (MDH51 S9) exhibits much higher G′ values than EVA filled with MDH alone (MDH60). However, both composites are plotted in regime II, i.e.

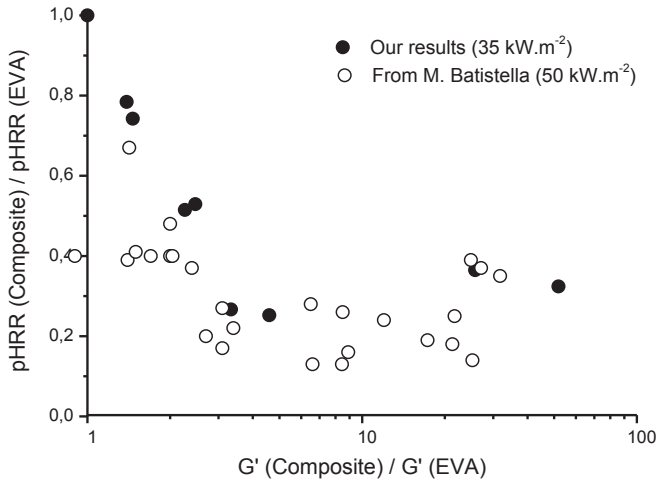

Fig. 7. Change in pHRR versus G′ for EVA filled with various mineral fillers (our work and Batistella's results [45]).

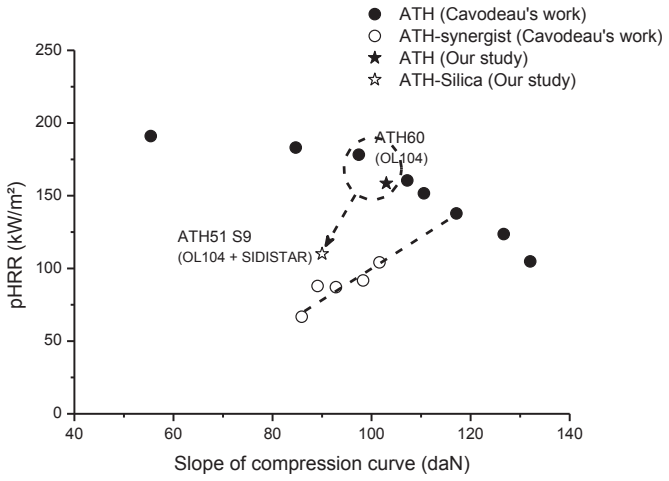

Fig. 8. Second peak of heat release rate versus slope of compression curve for residues prepared from different formulations used in Cavodeau's work [37], ATH60 and ATH51 S9 (our study).

pHRR is no longer dependent on G'. Therefore, no change in pHRR can be noted. But, it would be interesting to assess the combination of MDH and silica at low filler content (corresponding to regime I).

4.2. Resistance of barrier layer

Cavodeau et al. have recently shown that œdometric compression tests on filler powders (before their incorporation into EVA) allow predicting the occurrence of layer breakdown due to the pressure from pyrolytic gases [37]. The tested formulations were flame retarded by 60 wt% of ATH alone or 50 wt% of ATH and 10 wt% of non-hydrated fillers including SIDISTAR T120, i.e. these formulations were very close to the formulations tested in our study. The authors observed two specific behaviors. For formulations containing only ATH, lower is the slope measured in compression test, earlier is the barrier layer breakdown and higher is the pHRR 2. This result shows that a better compactness of the filler (measured by compression test) allows a more resistant protective layer. In contrast, in presence of some additives (like silica), a lower slope measured in the compression test leads to a later barrier breakdown and to a reduced second pHRR. This is explained by the slight swelling of the layer observed during cone calorimeter test. A low slope during compression test may allow the barrier layer to expand (rather than to break). Such (slightly) expanded layer is more efficient to insulate the underlying polymer. In all cases, the replacement of a small fraction of ATH by a non-hydrated mineral additive (among those studied) leads to a more resistant protective layer, limiting the second peak of heat release rate.

Residues from ATH60 and ATH51 S9 were tested according to the same procedure (Fig. 8). The second pHRR (pHRR 2) for EVA filled with 51 wt% of ATH and 9 wt% of silica almost vanished at 50 kW/m^2. It was approximately assessed to 110 kW/m^2. Residue from ATH60 exhibits a slightly higher pHRR 2 than the same formulation studied in Cavodeau's work and a similar slope of the compression curve. Replacing a small fraction of ATH by silica leads to a decrease of both pHRR 2 and slope of compression. This trend is qualitatively the same as in Cavodeau's work. According to the previous interpretation, this means that addition of non-hydrated fillers can lead to a mineral layer able to deform or flex to some degree without breaking. Since the breakdown of the barrier layer can be delayed or avoided completely, the peak of heat release rate is reduced or disappears.

5. Conclusion

This study has focused on evaluation of possible benefits of combining silica and ATH to improve the flame retardancy of EVA compounds. Some benefits have been observed, when the burning behavior of the compound includes the formation of a protective barrier layer; this is mostly the case for filler content of the order of 60 wt%. For low filler content the formation of a continuous protective layer may not be easily possible.

In cone calorimeter measurements, the presence of silica in the compound does not reduce significantly the first peak of heat release rate but leads to reduction or complete suppression of the second peak of heat release rate. The second peak can be related to the existence or breakdown of an insulating barrier layer. The effect is observed at all heat fluxes, but it is stronger at lower heat flux. At 75 kW/m^2, only a decrease in the second peak of the HRR is observed, while it disappears nearly completely at lower heat flux. At 25 kW/m^2, the integrity of the insulating barrier layer is maintained during combustion and allows incomplete decomposition of the copolymer.

Our observations are also discussed in view of recent results on filled EVA compounds. In particular, the first pHRR seems to be controlled by the rheological properties of the material. The breakdown of the protective layer is assumed to be mainly related to the packing of particles in the layer. Both peaks can be predicted by specific tests (respectively, rheological tests at processing temperature, and œdometric compression measurements on filler powders).

These results are essentially in agreement with those of Gallo et al. about SBR filled with ATH and SIDISTAR [31]. In their work, these authors used gravimetric gas sorption measurements to show the influence of SIDISTAR on the gas diffusion into the material. Such measurements on the residues (and not on the initial specimen) would be very useful to better characterize the role of SIDISTAR to improve the barrier effect of the mineral layer to pyrolytic gases diffusion.

Higher flame retardancy may be possible by combining non-hydrated and hydrated fillers. To identify combinations of metal hydroxides and silica fillers with optimized organization for the formation of an insulating and resistant barrier layer (in terms of their particle properties and loading) can help to produce highly flame retarded EVA compounds.

References

[1] M.S. Cross, P.A. Cusack, P.R. Hornsby, Effects of tin additives on the flammability and smoke emission characteristics of halogen-free ethylene-vinyl acetate copolymer, Polym. Degrad. Stab. 79 (2003) 309–318.

[2] S. Bourbigot, M. Le Bras, R. Leeuwendal, K.K. Shen, D. Schubert, Recent advances in the use of zinc borates in flame retardancy of EVA, Polym. Degrad. Stab. 64 (1999) 419–425.

[3] F. Carpentier, S. Bourbigot, M. Le Bras, R. Delobel, M. Foulon, Charring of fire retarded ethylene vinyl acetate copolymer – magnesium hydroxide/zinc borate formulations, Polym. Degrad. Stab. 69 (2000) 83–92.

[4] F. Carpentier, S. Bourbigot, M. Le Bras, R. Delobel, Rheological investigations in fire retardancy : application to ethylene vinyl-acetate copolymer-magnesium hydroxide/zinc borate formulations, Polym. Int. 49 (2000) 1216–1221.

[5] A. Durin-France, L. Ferry, J.-M. Lopez-Cuesta, A. Crespy, Magnesium hydroxide/zinc borate/talc compositions as flame-retardants in EVA copolymer, Polym. Int. 49 (2000) 1101–1105.

[6] Z. Li, B. Qu, Flammability characterization and synergistic effects of expandable graphite with magnesium hydroxide in halogen-free flame-retardant EVA blends, Polym. Degrad. Stab. 81 (2003) 401–408.

[7] G. Beyer, Flame retardancy of nanocomposites based on organoclays and carbon nanotubes with aluminium trihydrate, Polym. Adv. Technol. 17 (2006) 218–225.

[8] L. Ye, Q. Wu, B. Qu, Synergistic effects and mechanism of multiwalled carbon nanotubes with magnesium hydroxide in halogen-free flame retardant EVA/MH/MWNT nanocomposites, Polym. Degrad. Stab. 94 (2009) 751–756.

[9] L. Ye, P. Ding, M. Zhang, B. Qu, Synergistic Effects of Exfoliated LDH with Some Halogen-Free Flame Retardants in LDPE/EVA/HFMH/LDH Nanocomposites, J. Appl. Polym. Sci. 107 (2008) 3694–3701.

[10] H. Gui, X. Zhang, W. Dong, Q. Wang, J. Gao, Z. Song, J. Lai, Y. Liu, F. Huang, J. Qiao, Flame retardant synergism of rubber and $Mg(OH)_2$ in EVA composites, Polymer 48 (2007) 2537–2541.

[11] H. Gui, X. Zhang, W. Dong, J. Gao, Z. Song, J. Lai, Y. Liu, F. Huang, J. Qiao, Q. Wang, Effect of rubbers on the flame retardancy of eva/ultrafine fully vulcanized powdered rubber/nanomagnesium hydroxide ternary composites, Polym. Compos. 28 (2007) 479–483.

[12] H. Gui, X. Zhang, Y. Liu, W. Dong, Q. Wang, J. Gao, Z. Song, J. Lai, J. Qiao, Effect of dispersion of nano-magnesium hydroxide on the flammability of flame retardant ternary composites, Compos. Sci. Technol. 67 (2007) 974–980.

[13] J. Zilberman, T.R. Hull, D. Price, G.J. Milnes, F. Keen, Flame retardancy of some ethylene-vinyl acetate copolymer-based formulations, Fire Mater. 24 (2000) 159–164.

[14] A. Riva, G. Camino, L. Fomperie, P. Amigouët, Fire retardant mechanism in intumescent ethylene vinyl acetate compositions, Polym. Degrad. Stab. 82 (2003) 341–346.

[15] J.-P. Lv, W.-H. Liu, Flame Retardancy and Mechanical properties of EVA nanocomposites based on magnesium hydroxide nanoparticles/microencapsulated red phosphorus, J. Appl. Polym. Sci. 105 (2007) 333–340.

[16] L. Wang, X. Wu, C. Wu, J. Yu, G. Wang, P. Jiang, Study on the flame retardancy of EVM/magnesium hydroxide composites optimized with a flame retardant containing phosphorus and silicon, J. Appl. Polym. Sci. 121 (2011) 68–77.

[17] C.-M. Jiao, X.-L. Chen, Synergistic flame retardant effect of cerium oxide in ethylene-vinyl acetate/aluminum hydroxide blends, J. Appl. Polym. Sci. 116 (2010) 1889–1893.

[18] C.-M. Jiao, X.-L. Chen, Influence of fumed silica on the flame-retardant properties of ethylene vinyl acetate/aluminum hydroxide composites, J. Appl. Polym. Sci. 120 (2011) 1285–1289.

[19] H. Huang, M. Tian, L. Liu, Z. He, Z. Chen, L. Zhang, Effects of silicon additive as synergists of $Mg(OH)_2$ on the flammability of ethylene vinyl acetate copolymer, J. Appl. Polym. Sci. 99 (2006) 3203–3209.

[20] M. Fu, B. Qu, Synergistic flame retardant mechanism of fumed silica in ethylene-vinyl acetate/magnesium hydroxide blends, Polym. Degrad. Stab. 85 (2004) 633–639.

[21] L. Clerc, L. Ferry, E. Leroy, J.-M. Lopez-Cuesta, Influence of talc physical properties on the fire retarding behaviour of (ethylene-vinyl acetate copolymer/magnesium hydroxide/talc) composites, Polym. Degrad. Stab. 88 (2005) 504–511.

[22] M.A. Cardenas, D. Garcia-Lopez, I. Gobernado-Mitre, J.C. Merino, J.M. Pastor, J. De, D. Martinez, J. Barbeta, D. Calveras, Mechanical and fire retardant properties of EVA/clay/ATH nanocomposites – Effect of particle size and surface treatment of ATH filler, Polym. Degrad. Stab. 93 (2008) 2032–2037.

[23] G. Beyer, Flame retardant properties of EVA-nanocomposites and improvements by combination of nanofillers with aluminium trihydrate, Fire Mater. 25 (2001) 193–197.

[24] L. Haurie, A.I. Fernandez, J.I. Velasco, J.-M. Chimenos, J.-M. Lopez-Cuesta, F. Espiell, Thermal stability and flame retardancy of LDPE/EVA blends filled with synthetic hydromagnesite/aluminium hydroxide/montmorillonite and magnesium hydroxide/aluminium hydroxide/montmorillonite mixtures, Polym. Degrad. Stab. 92 (2007) 1082–1087.

[25] F. Laoutid, P. Gaudon, J.-M. Taulemesse, J.M. Lopez-Cuesta, J.I. Velaco, A. Piechaczyk, Study of hydromagnesite and magnesium hydroxide based fire retardant systems for ethylene-vinyl acetate containing organo-modified montmorillonite, Polym. Degrad. Stab. 91 (2006) 3074–3082.

[26] A.B. Morgan, J.M. Cogen, R.S. Opperman, J.D. Harris, The effectiveness of magnesium carbonate-based flame retardants for poly(ethylene-co-vinyl acetate) and poly(ethylene-co-ethyl acrylate), Fire Mater. 31 (2007) 387–410.

[27] A. Szep, A. Szabo, N. Toth, P. Anna, G. Marosi, Role of montmorillonite in flame retardancy of ethylene-vinyl acetate copolymer, Polym. Degrad. Stab. 91 (2006) 593–599.

[28] Y. Zhang, Y. Hu, L. Song, J. Wu, S. Fang, Influence of Fe-MMT on the fire retarding behavior and mechanical property of (ethylene-vinyl acetate copolymer/magnesium hydroxide) composite, Polym. Adv. Technol. 19 (2008) 960–966.

[29] J. Zhang, J. Hereid, M. Hagen, D. Bakirtzis, M.A. Delichatsios, A. Fina, A. Castrovinci, G. Camino, F. Samyn, S. Bourbigot, Effects of nanoclay and fire retardants on fire retardancy of a polymer blend of EVA and LDPE, Fire Saf. J. 44 (2009) 504–513.

[30] G. Schmauks, B. Friede, Amorphous Silicon Dioxide as Additive to Improve the Fire Retardancy of Polyamides, in: R. Hull (Ed.), Fire Retardancy of Polymers: New Strategies and Mechanisms, Royal Society of Chemistry, 2009.

[31] E. Gallo, B. Schartel, G. Schmaucks, K. Von der Ehe, M. Boehning, The effect of well-dispersed amorphous silicon dioxide in flame-retarded styrene butadiene rubber, plastics, Rubber Compos. 42 (2013) 34–42.

[32] G. Schmaucks, J.O. Roszinski, High Performance Engineering Plastics and Additive for Use in Engineering Plastics, European Patent 1824917, 2009.

[33] B. Schartel, G. Schmaucks, J.O. Roszinski: NO 20084323.

[34] R.E. Lyon, R.N. Walters, Pyrolysis combustion flow calorimetry, J. Anal. Appl. Pyrolysis 71 (2004) 27–46.

[35] C. Huggett, Estimation of rate of heat release by means of oxygen consumption measurements, Fire Mater. 4 (1980) 61–65.

[36] R. Sonnier, H. Vahabi, L. Ferry, J.-M. Lopez-Cuesta, Pyrolysis-combustion flow calorimetry: a powerful tool to evaluate the flame retardancy of polymers, in: C. Wilkie (Ed.), Fire and Polymers VI: New Advances in Flame Retardant Chemistry and Science, ACS, December 2012.

[37] F. Cavodeau, R. Sonnier, B. Otazaghine, J.-M. Lopez-Cuesta, C. Delaite, A predictive method of the barrier effect during cone calorimeter tests of aluminium hydroxide/ethylene-vinyl acetate copolymer composites, Polym. Degrad. Stab. 120 (2015) 23–31.

[38] R. Sonnier, L. Bokobza, N. Concha-Lozano, Influence of multiwall carbon nanotubes (MWCNT) dispersion on ignition of poly(dimethylsiloxane)-MWCNT composites, Polym. Adv. Technol. 26 (2015) 277–286.

[39] B. Schartel, T.R. Hull, Development of fire-retarded materials – Interpretation of cone calorimeter data, Fire Mater. 31 (2007) 327–354.

[40] E.S. Oztekin, S.B. Crowley, R.E. Lyon, S.I. Stoliarov, P. Patel, T.R. Hull, Sources of variability in fire test data: a case study on poly(aryl ether ether ketone) (PEEK), Combust. Flame 159 (2012) 1720–1731.

[41] J. Courtat, F. Melis, J-M. Taulemesse, V. Bounor-Legaré, R. Sonnier, L. Ferry, P. Cassagnau, Fire retardancy of polypropylene/silica composites, Polymer Degradation and Stability, submitted.

[42] T. Kashiwagi, J.W. Gilman, K.M. Butler, R.H. Harris, J.R. Shields, A. Asano, Flame retardant mechanism of silica gel/silica, Fire Mater. 24 (2000) 277–289.

[43] T. Kashiwagi, J.R. Shields, R.H. Harris, R.D. Davis, Flame-retardant mechanism of silica: Effects of resin molecular weight, J. Appl. Polym. Sci. 87 (2003) 1541–1553.

[44] T. Kashiwagi, M. Mu, K. Winey, B. Cipriano, S.R. Raghavan, S. Pack, M. Rafailovich, Y. Yang, E. Grulke, J. Shields, R. Harris, J. Douglas, Relation between the viscoelastic and flammability properties of polymer nanocomposites, Polymer 49 (2008) 4358–4368.

[45] M. Batistella, B. Otazaghine, R. Sonnier, A.-S. Caro-Bretelle, C. Petter, J.-M. Lopez-Cuesta, Fire retardancy of ethylene vinyl acetate/ultrafine kaolinite composites, Polym. Degrad. Stab. 100 (2014) 54–62.